CrossMark

Numerical investigation into dynamic behavior of electrostatically-actuated circular clamped micro-plate subject to squeeze-film damping effect

Chin-Chia Liu[1]

Abstract The analysis of electrostatically-actuated MEMS devices is complicated since structural deformation alters the nonlinear electrostatic force, which in turn redistributes and modifies the electrostatic coupling effect. The analysis is further complicated by the nonlinear squeeze-film damping effect exerted by the air film between the deformable diaphragm and the fixed substrate. Accordingly, the present study performs a numerical investigation into the effect of this squeeze-film damping phenomenon on the dynamic behavior of a MEMS device incorporating a circular clamped micro-plate. The deflection behavior of the micro-plate is described using an analytical model based on a linearized isothermal compressible Reynolds equation and a sealed pressure boundary condition. In performing the simulations, the model is solved using a hybrid differential transformation and finite difference scheme. The simulations focus specifically on the effects of the residual stress, actuation voltage and excitation frequency on the dynamic response of the membrane.

1 Introduction

Electrostatically-actuated microelectromechanical systems (MEMS) devices are used widely throughout industry for such applications as microphones (Liu et al. 2008) and micro-pumps (Jiankang and Lijun 2006). Typical MEMS devices feature a parallel-plate capacitor, in which the upper electrode is actuated electrically and the corresponding deformation is detected by measuring the resulting capacitive change. In order to increase the actuation efficiency and improve the detection sensitivity, the distance between the electrodes should be minimized and the overlapping area between them maximized.

However, under such conditions, the air gap between the two electrodes results in a significant squeeze-film damping effect as the upper electrode deforms toward the lower substrate. In practice, this damping effect must be taken into account in designing the device and predicting its performance under realistic actuation conditions. In many previous studies, the squeeze-film damping effect has been examined by means of finite element method (FEM) simulations (Homentcovschi et al. 2010; Nigro et al. 2010, 2012). Such methods yield highly accurate solutions. However, they lack explicit physical meaning and are both time-consuming and computationally expensive. As a result, they are impractical for many design optimization tasks (Younis et al. 2003; Nayfeh et al. 2005). Lumped models are simple and have explicit physical meaning. However, they have a lower accuracy than FEM models. As a result, it has been suggested that analytical models represent a more suitable method for exploring the physical characteristics and nonlinear dynamic behavior of MEMS structures (Liu and Chen 2013). Nayfeh and Younis (2004) investigated the squeeze-film damping effect in a MEMS device containing a rectangular micro-plate. In performing the analysis, the damping effect and micro-plate deformation were modeled using a linearized Reynolds equation and classical plate theory (CPT), respectively. Liu and Wang (2014) proposed an analytical model based on a nonlinear deflection equation and a Reynolds equation for investigating the dynamic response of an electrically-actuated clamped–clamped micro-beam subject to squeeze-film damping. Younis

✉ Chin-Chia Liu
ccliu@cc.ncue.edu.tw

1 Department of Industrial Education and Technology, National Changhua University of Education, Bao-Shan Campus, Number 2, Shi-Da Road, Changhua 500, Taiwan, R.O.C.

(2004) presented a hybrid numerical/analytical method for simulating MEMS systems subject to squeeze-film damping effects in multi-physics fields.

The present study performs a numerical investigation into the effect of the squeeze-film damping phenomenon on the dynamic behavior of a MEMS device incorporating a circular clamped micro-plate. In performing the simulations, the nonlinear governing equation of motion of the micro-plate is solved using a hybrid differential transformation and finite difference method.

2 Problem formulation

2.1 Governing equation for circular micro-plate

Figure 1 presents a schematic illustration of the MEMS device considered in the present study. As shown, the device comprises a lower fixed electrode, a dielectric spacer, and an upper deformable circular micro-plate. The governing equation of the micro-plate subject to both a residual stress force within the plate and a squeeze-film damping effect between the plate and the lower electrode has the form (Chen et al. 2009)

$$\rho h \frac{\partial^2 u}{\partial t^2} + \left(\frac{Eh^3}{12(1-\upsilon^2)}\right)\left(\frac{\partial^2}{\partial r^2} + \frac{1}{r}\frac{\partial}{\partial r}\right)\left(\frac{\partial^2 u}{\partial r^2} + \frac{1}{r}\frac{\partial u}{\partial r}\right)$$
$$- T_r h \left(\frac{\partial^2 u}{\partial r^2} + \frac{1}{r}\frac{\partial u}{\partial r}\right) = \frac{\varepsilon_0 V(t)^2}{2(G-u)^2} - P_p, \qquad (1)$$

where ε_0, h, υ, E and G are the permittivity of free space, the thickness of the micro-plate, the Poisson ratio of the micro-plate material, the Young's modulus of the micro-plate material and the initial gap height between the micro-plate and the lower electrode, respectively. In addition, ρ is the density of the micro-plate material, and u is the transverse deflection of the micro-plate at a radial distance r from the center. Note that u is a function only of the position r and the time t, i.e., $u = u(r, t)$. In other words, for a given value of r and t, the transverse deflection of the plate is independent of the polar coordinate, θ. Finally, T_r is the

residual stress within the plate, P_p is the net pressure within the air gap, and $V(t)$ is the actuation voltage. In the present study, the micro-plate is actuated by a hybrid DC/AC voltage scheme, i.e., $V(t) = V_{DC} + V_{AC}\sin(\omega t)$, where V_{DC} is the DC polarization voltage, V_{AC} is the magnitude of the AC voltage, and ω is the excitation frequency.

The boundary conditions for the governing equation of motion of the micro-plate are given as follows:

$$u(r, t) = \frac{\partial u(r, t)}{\partial r} = 0 \ \text{ at } r = \pm R, \qquad (2)$$

where R is the radius of the micro-plate.

Meanwhile, the initial condition is given as

$$u(r, 0) = \frac{\partial u(r, 0)}{\partial t} = 0. \qquad (3)$$

In the present study, the squeeze-film damping effect within the air gap is modeled using the linearized compressible gas-film Reynolds equation (Liu and Wang 2014), which has the form

$$\frac{\partial^2 P_p}{\partial r^2} + \frac{1}{r}\frac{\partial P_p}{\partial r} = \frac{12\mu}{P_a G^3}\left(G\frac{\partial P_p}{\partial t} + P_a \frac{\partial h_p}{\partial t}\right), \qquad (4)$$

where h_p and μ represent the variable distance between the two electrodes (i.e., $h_p = G - u$) and the effective viscosity of the air in the air gap, respectively. Based on the Knudsen number (K_n), defined as the ratio of the mean free path of the air particles to the film thickness (λ/h_p) (note that λ is the molecular mean free path length and has a value of $\lambda = 0.064\,\mu m$ for air.), air flows can be divided into four regimes, namely continuum flow when ($K_n < 0.01$), slip flow ($0.01 < K_n < 0.1$), transitional flow ($0.1 < K_n < 10$) and free molecular flow ($K_n > 10$) (Nayfeh and Younis 2004). In many MEMS devices, K_n is close to the non-continuum regime. To take account of the correction required for the slip boundary condition, the effective viscosity of the air should be computed as $\mu = \mu_0/(1 + 6K_n)$, where μ_0 is the absolute air viscosity (Krylov 2007). Furthermore, the net pressure in the air gap can be expressed as $P_p = P - P_a$, where P is the absolute pressure in the gap

Fig. 1 Schematic illustration showing electrostatic actuation of circular micro-plate
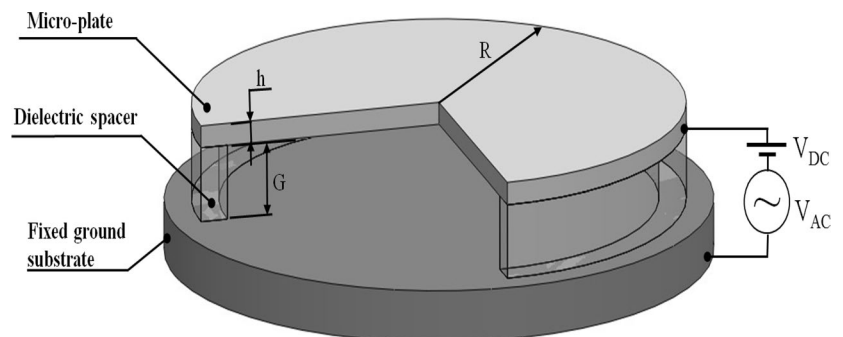
and P_a is the ambient pressure. Finally, the pressure boundary conditions are given as follows:

$$P_p(R, t) = 0, \quad \frac{\partial P_p(0, t)}{\partial r} = 0. \tag{5}$$

2.2 Dimensionless governing equation and decomposition by hybrid method

For analytical convenience, let the following non-dimensional variables (denoted by a hat) be introduced:

$$\bar{u} = \frac{u}{G}, \ \bar{r} = \frac{r}{R}, \ \bar{t} = \frac{t}{\bar{T}}, \ \bar{\omega} = \omega\bar{T}, \ \bar{P} = \frac{P_p}{P_a} \text{ and } \bar{H} = \frac{h_p}{G}. \tag{6}$$

As shown, the transverse displacement u of the membrane is normalized with respect to the initial gap between the electrodes, the radial distance quantity r is normalized with respect to the radius of the circular micro-plate, and the time t is normalized with respect to the constant $\bar{T}$, where $\bar{T}$ is defined as $\bar{T} = \sqrt{\rho h R^4 / D}$ (note that D is the flexural rigidity of the plate, i.e., $D = Eh^3 / 12(1 - \upsilon^2)$). Finally, the excitation frequency ω is normalized by taking the product of ω and the time constant $\bar{T}$.

Let the following parameters be additionally defined:

$$Q^* = \frac{R^4 \varepsilon_0}{2DG}, \ T_r^* = \frac{T_r^4 R^2 h}{D}, \ A^* = \frac{P_a R^4}{DG}. \tag{7}$$

Substituting Eqs. (6) and (7) into Eqs. (1), (2) and (3), the dimensionless governing equation of motion for the circular micro-plate is obtained as

$$\frac{\partial^4 \bar{u}}{\partial \bar{r}^4} + \frac{\partial^2 \bar{u}}{\partial \bar{t}^2} + \frac{2}{\bar{r}} \frac{\partial^3 \bar{u}}{\partial \bar{r}^3} - \frac{1}{\bar{r}^2} \frac{\partial^2 \bar{u}}{\partial \bar{r}^2} + \frac{1}{\bar{r}^3} \frac{\partial \bar{u}}{\partial \bar{r}} - T_r^* \frac{\partial^2 \bar{u}}{\partial \bar{r}^2} - T_r^* \frac{1}{\bar{r}} \frac{\partial \bar{u}}{\partial \bar{r}}$$
$$= \frac{Q^* [V_{DC} + V_{AC} \sin(\bar{\omega}\bar{t})]^2}{(1 - \bar{u})^2} - \bar{P} A^*. \tag{8}$$

The corresponding dimensionless boundary conditions are given as follows:

$$\bar{u}(\bar{r}, \bar{t}) = \frac{\partial \bar{u}(\bar{r}, \bar{t})}{\partial \bar{r}} = 0 \text{ at } \bar{r} = \pm 1. \tag{9}$$

Finally, the initial condition is equal to

$$\bar{u}(\bar{r}, 0) = \frac{\partial \bar{u}(\bar{r}, 0)}{\partial \bar{t}} = 0. \tag{10}$$

Substituting Eq. (6) into Eqs. (4) and (5), the dimensionless linearized one-dimensional Reynolds equation is obtained as follows:

$$\frac{\partial^2 \bar{P}}{\partial \bar{r}^2} + \frac{1}{\bar{r}} \frac{\partial \bar{P}}{\partial \bar{r}} = \sigma \left(\frac{\partial \bar{P}}{\partial \bar{t}} - \frac{\partial \bar{u}}{\partial \bar{t}} \right), \tag{11}$$

where $\sigma = 12\mu R^2 / P_a G^2 \bar{T}$ is the well-known squeeze number.

In the present study, the nonlinear governing equation of motion for the circular micro-plate [Eq. (8)] is solved using the hybrid differential transformation and finite difference method described in Liu and Wang (2014). The solution procedure commences by discretizing the equation of motion with respect to the time domain t using the differential transformation method, i.e.,

$$T\left[\frac{\partial^4 \bar{u}}{\partial \bar{r}^4}\right] = \frac{d^4 U(\bar{r}, k)}{d\bar{r}^4}, \ T\left[\frac{\partial^2 \bar{u}}{\partial \bar{t}^2}\right] = \frac{(k+1)(k+2)}{H^2} U(\bar{r}, k+2),$$
$$T\left[\frac{2}{\bar{r}} \frac{\partial^3 \bar{u}}{\partial \bar{r}^3}\right] = \frac{2}{\bar{r}} \frac{d^3 U(\bar{r}, k)}{d\bar{r}^3}. \tag{12}$$

Having applied the differential transformation method to the governing equation, associated boundary conditions and initial condition of the circular micro-plate, the transverse displacement of the micro-plate is then discretized spatially in the radial direction using the finite difference approximation method based on fourth-order and second-order accurate central difference formulae.

3 Results and discussion

Table 1 summarizes the material and geometry parameters considered in the present simulations. Figure 2 shows the variation of the dimensionless center-point deflection of the circular micro-plate with the applied actuation voltage for three different values of the residual stress. Note that the micro-plate is actuated by a DC voltage only (i.e., the AC driving voltage is not applied). As the residual stress increased from a negative value to positive values, the pull-in voltage increased at the same time. Furthermore, the pull-in voltage of the blue line with negative residual stress ($T_r = -10$ MPa) was 13.7 V, the pull-in voltage of the red line without residual stress ($T_r = 0$ MPa) was 19.3 V and the pull-in voltage of the green line with positive residual stress ($T_r = 10$ MPa) was 23.5 V. It is seen that for all three values of the residual stress, the center-point of the plate

Table 1 Material and geometry parameters considered in present simulations

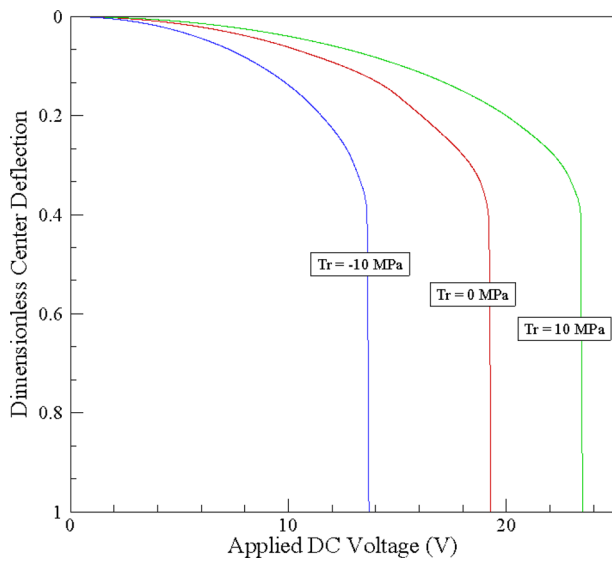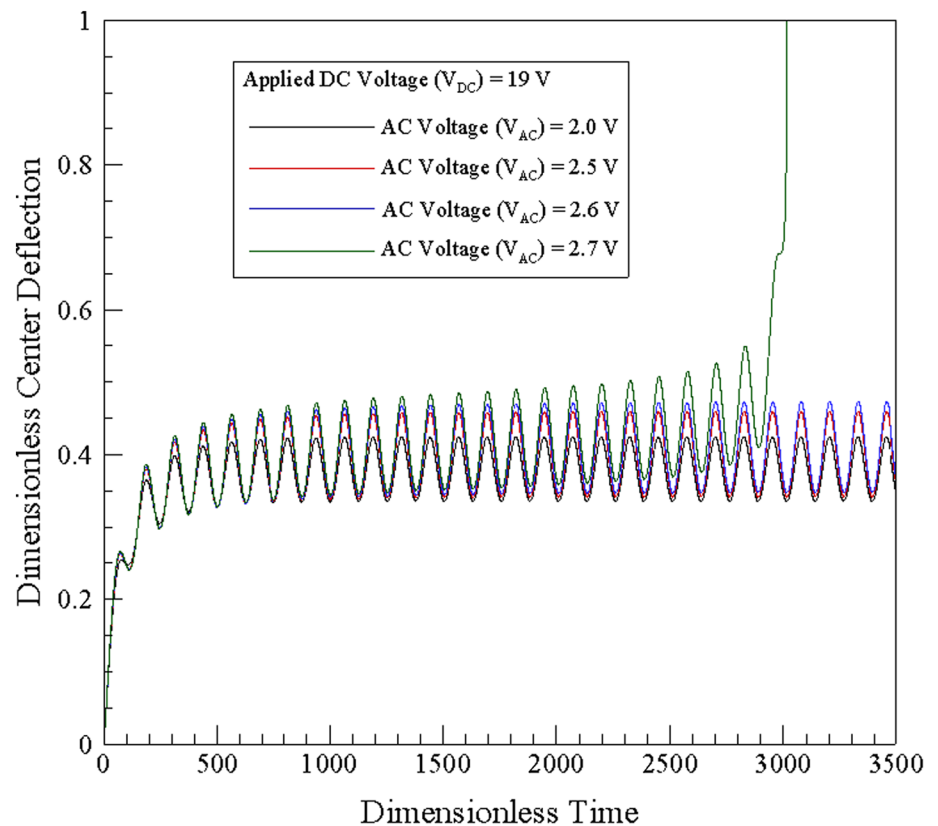| Parameters/symbol/unit	Value
Young's modulus (E) (GPa)	130
Poisson's Ratio (ν)	0.23
Density (ρ) (Kg/m³)	2.33×10^3
Permittivity of free space (ε_0) (F/m)	$8.8541878 \times 10^{-12}$
Thickness of circular micro-plate (h) (μm)	1
Initial gap (G) (μm)	1
Radius of circular micro-plate (R) (μm)	100
Ambient pressure (P_a) (bar)	1

Fig. 2 Variation of dimensionless center-point displacement with DC voltage (note that AC voltage is not applied)

lower substrate. It is further noted, that the critical voltage at which this "pull-event" occurs increases as the residual stress changes from a negative (i.e., $T_r = -10$ MPa) value to a positive (i.e., $T_r = 10$ MPa) value.

Figure 3 shows the variation of the center-point deflection of the micro-plate over time given a constant DC voltage of 19 V and AC voltages ranging from 2.0 to 2.7 V. It is seen that for all values of the AC voltage, the center-point deflection increases irregularly over the first 0–800 dimensionless time units. Hence, it is inferred that the DC driving voltage is unstable during the initial stages of the actuation period. In addition, it is observed that as the applied AC voltage increases, the center-point deflection of the micro-beam increases nonlinearly due to an electrostatic coupling effect. For AC voltages of less than 2.6 V, the micro-plate oscillates in a stable manner about the deflection point. However, for an AC voltage of 2.7 V, the pull-in phenomenon occurs and the micro-plate collapses, causing the center-point of the plate to make transient contact with the lower electrode.

Figure 4 shows the phase portraits of the circular micro-plate for a constant DC voltage of 19 V and AC voltages of 2.6 and 2.7 V, respectively. The results show that for an AC voltage of 2.6 V, the system exhibits a stable behavior, i.e., the size of the orbit remains approximately constant over time. However, for an actuating voltage of 2.7 V, the size

progressively deflects toward the lower substrate as the actuation voltage is increased. However, at a certain critical value of the actuation voltage, the micro-plate collapses, causing the center-point to make transient contact with the

Fig. 3 Variation of dimensionless center-point displacement over time for constant DC voltage and AC voltages ranging from 2.0–2.7 V (note that the DC voltage is assumed to have 19 V, and $\bar{\omega} = 1$)

Fig. 4 Phase portraits for circular micro-plate given constant DC voltage of 19 V and AC voltages of 2.6 and 2.7 V (note that the $\bar{\omega} = 1$)
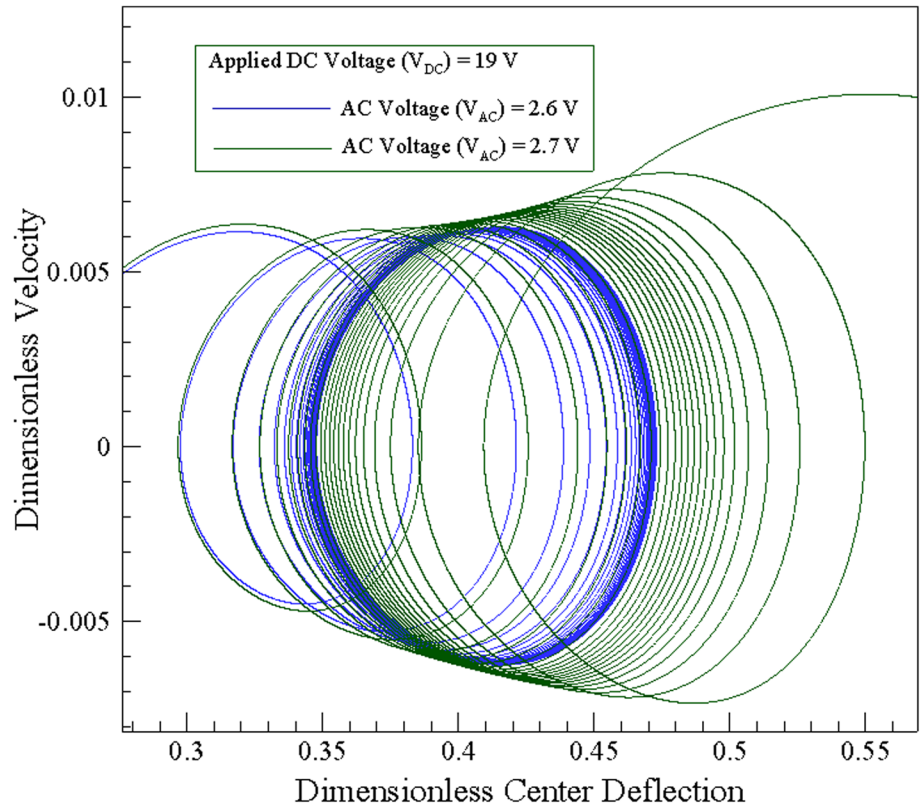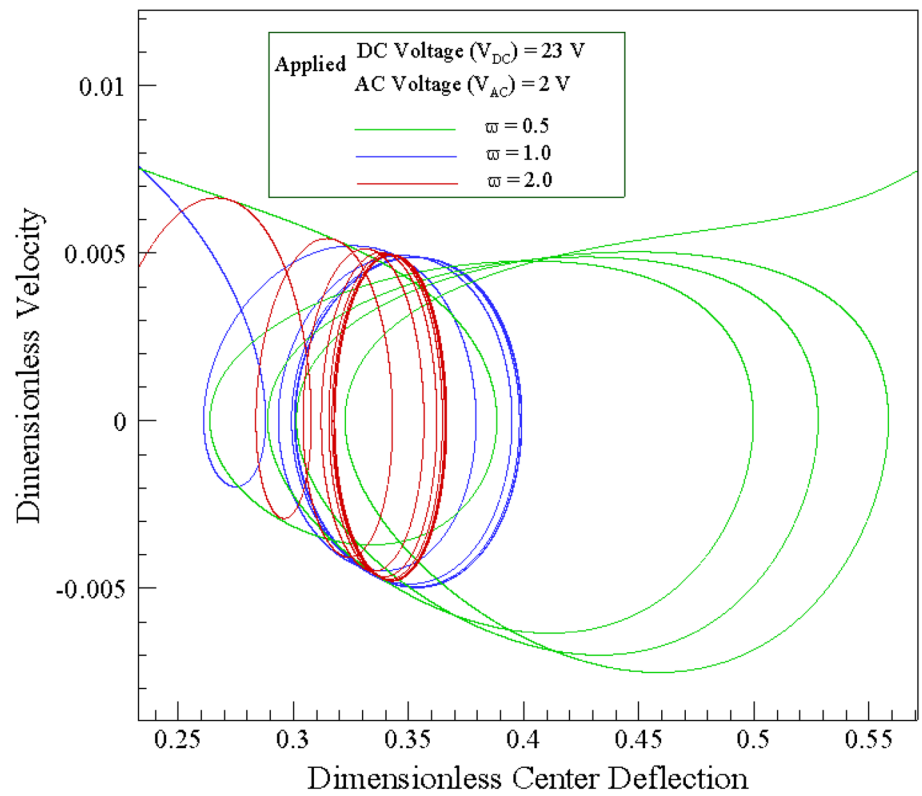

Fig. 5 Phase portraits for circular micro-plate given constant DV voltage of 23 V, constant AC voltage of 2 V and dimensionless excitation frequencies ranging from 0.5 to 2.0

of the orbit gradually increases until the system becomes unstable and the pull-in event occurs.

Figure 5 presents the phase portraits of the oscillating micro-plate given constant DC and AC voltages of 23 and 2 V, respectively, and dimensionless excitation frequencies ranging from 0.5 to 2.0. It is seen that for dimensionless excitation frequencies of 1.0 and 2.0, the micro-plate exhibits a stable periodic response. However, for the lowest excitation frequency of 0.5, the system gradually loses stability and the circular micro-plate collapses onto the lower substrate.

4 Conclusions

The present study has used a hybrid numerical scheme comprising the differential transformation method and the finite difference method to investigate the nonlinear dynamic behavior of an electrostatically-actuated circular micro-plate subject to a squeeze-film damping effect. The results have shown that given a DC driving voltage, the pull-in voltage increases as the residual stress within the micro-plate changes from a compressive stress to a tensile stress. Furthermore, it has been shown that the use of an AC actuating voltage in addition to the DC driving voltage provides an effective means of tuning the dynamic response of the circular micro-plate. Finally, it has been shown that the stability of the circular micro-plate reduces as the magnitude of the AC voltage increases or the excitation frequency reduces.

Appendix

Elementary symbol table

Symbol	Parameters
A^*	Dimensionless parameter
b	Width of beam
D	Flexural rigidity of the plate
E	Young's modulus
G	Initial gap
H	Time interval
$\bar{H}$	Dimensionless distance between the gap
h	Thickness of the micro-plate

Symbol	Parameters
h_p	Variable distance between the gap $(h_p = G - u)$
K_n	Knudsen number (λ / h_p)
P	Absolute pressure
P_a	Ambient pressure
P_p	Net pressure $(P_p = P - P_a)$
$\bar{P}$	Dimensionless pressure
Q^*	Dimensionless parameter
R	Radius of the micro-plate
$\bar{r}$	Dimensionless radial distance
T	Differential transformation operation
T	Differential transformation operation
$\bar{T}$	Dimensionless time
T_r^*	Dimensionless parameter
t	Time
U	Differential transformed function of $\bar{u}$
u	Transverse deflection
$\bar{u}$	Dimensionless deflection
V_{DC}	The DC voltage
V_{AC}	The AC voltage
Greek symbols	
θ	Polar coordinate
ω	Excitation frequency
$\bar{\omega}$	Dimensionless frequency
λ	The molecular mean free path length
μ	Effective viscosity
μ_0	Absolute viscosity
υ	Poisson's Ration
ρ	Density
ε_0	Permittivity of free space
σ	Squeeze number

References

Chen CK, Lai HY, Liu CC (2009) Nonlinear micro circular plate analysis using hybrid differential transformation/finite difference method. Comput Model Eng Sci (CMES) 40(2):155–174

Homentcovschi D, Murray BT, Miles RN (2010) An analytical formula and FEM simulations for the viscous damping of a periodic perforated MEMS microstructure outside the lubrication approximation. Microfluid Nanofluid 9(4–5):865–879

Jiankang W, Lijun L (2006) Liquid-solid coupled system of micropump. Acta Mech Solida Sin 19(1):40–49

Krylov S (2007) Lyapunov exponents as a criterion for the dynamic pull-in instability of electrostatically actuated microstructures. Int J Non-Linear Mech 42(4):626–642

Liu CC, Chen CK (2013) Modeling and simulation of nonlinear micro-electromechanical circular plate. Smart Sci 1(1):59–63

Liu CC, Wang CC (2014) Numerical investigation into nonlinear dynamic behavior of electrically-actuated clamped–clamped micro-beam with squeeze-film damping effect. Appl Math Model 38(13):3269–3280

Liu J, Martin DT, Kadirvel K, Nishida T, Cattafesta L, Sheplak M, Mann BP (2008) Nonlinear model and system identification of a capacitive dual-backplate MEMS microphone. J Sound Vib 309(1):276–292

Nayfeh AH, Younis MI (2004) A new approach to the modeling and simulation of flexible microstructures under the effect of squeeze-film damping. J Micromech Microeng 14(2):170

Nayfeh AH, Younis MI, Abdel-Rahman EM (2005) Reduced-order models for MEMS applications. Nonlinear Dyn 41(1–3):211–236

Nigro S, Pagnotta L, Pantano MF (2010) Evaluation of the squeeze-film damping effects in MEMS perforated plates. In: 8th IASME/WSEAS international conference on fluid mechanics and aerodynamics, Taipei, Taiwan, pp 314–319

Nigro S, Pagnotta L, Pantano MF (2012) Analytical and numerical modeling of squeeze-film damping in perforated microstructures. Microfluid Nanofluid 12(6):971–979

Younis MI (2004) Modeling and simulation of microelectromechanical systems in multi-physics fields. Doctoral dissertation, Virginia Polytechnic Institute and State University

Younis MI, Abdel-Rahman EM, Nayfeh A (2003) A reduced-order model for electrically actuated microbeam-based MEMS. Microelectromech Syst J 12(5):672–680